frontiers | Frontiers in Earth Science

TYPE Original Research
PUBLISHED 11 November 2022
DOI 10.3389/feart.2022.1034704

OPEN ACCESS

EDITED BY
Qinzhuo Liao,
China University of Petroleum, China

REVIEWED BY
Ibrahim Mohamed,
Advantek Waste Management Services, United States
Ahmed Alsaihati,
Saudi Aramco, Saudi Arabia

*CORRESPONDENCE
Salaheldin Elkatatny,
elkatatny@kfupm.edu.sa

SPECIALTY SECTION
This article was submitted to Environmental Informatics and Remote Sensing,
a section of the journal
Frontiers in Earth Science

RECEIVED 01 September 2022
ACCEPTED 28 October 2022
PUBLISHED 11 November 2022

CITATION
Mahmoud AA, Gamal H, Elkatatny S and Chen W (2022), Real-time evaluation of the dynamic Young's modulus for composite formations based on the drilling parameters using different machine learning algorithms.
Front. Earth Sci. 10:1034704.
doi: 10.3389/feart.2022.1034704

Real-time evaluation of the dynamic Young's modulus for composite formations based on the drilling parameters using different machine learning algorithms

Ahmed Abdulhamid Mahmoud[1], Hany Gamal[1], Salaheldin Elkatatny[1]* and Weiqing Chen[2]

[1]Petroleum Engineering Department, College of Petroleum Engineering and Geosciences, King Fahd University of Petroleum and Minerals, Dhahran, Saudi Arabia, [2]Center for Integrative Petroleum Research, College of Petroleum Engineering and Geosciences, King Fahd University of Petroleum and Minerals, Dhahran, Saudi Arabia

The dynamic Young's modulus (E_{dyn}) is a parameter needed for optimizing different aspects related to oil well designing. Currently, E_{dyn} is determined from the knowledge of the formation bulk density, in addition to the shear and compressional velocities, which are not always available. This study introduces three machine learning (ML) models, namely, random forest (RF), adaptive neuro-fuzzy inference system with subtractive clustering (ANFIS-SC), and support vector regression (SVR), for estimation of the E_{dyn} from only the real-time available drilling parameters. The ML models were learned on 2054 datasets collected from Well-A and then tested and validated on 871 and 2912 datasets from Well-B and Well-C, respectively. The results showed that the three optimized ML models accurately predicted the E_{dyn} in the three oil wells considered in this study. The optimized SVR model outperformed both the RF and ANFIS-SC models in evaluating the E_{dyn} in all three wells. For the validation data, the E_{dyn} was assessed accurately with low average absolute percentage errors of 3.64%, 6.74%, and 1.03% using the optimized RF, ANFIS-SC, and SVR models, respectively.

KEYWORDS

dynamic Young's modulus, drilling parameters, machine learning models, real-time prediction, composite formation

1 Introduction

Rock static elastic properties are key parameters affecting *in situ* stress distribution prediction, hydraulic fracturing design, and wellbore stability (Labudovic, 1984; Lacy, 1997; Nes et al., 2005; Hammah et al., 2006; Fjaer et al., 2008). Nowadays, these static elastic properties are predicted using laboratory measurements (Barree et al., 2009) or empirical correlations which evaluated the static elastic parameters based on the dynamic elastic parameters predicted from the well log data (King, 1983; Brotons et al., 2016; Asef and Farrokhrouz, 2017; Karagianni et al., 2017).

Young's modulus is an important elastic property, and the static values of Young's modulus (E_{st}) could be predicted with high accuracy using laboratory measurement or predicted with empirical correlations developed to predict the E_{st}. Table 1 lists different empirical correlations suggested for estimation of E_{st} in different rock types.

The dynamic Young's modulus (E_{dyn}) which is required for E_{st} prediction by all empirical correlations in Table 1 is currently determined from acoustic velocities and rock density using Eq. 1 (Fjaer et al., 2008). The inputs required to estimate the E_{dyn} using Eq. 1 are obtained from the laboratory experiments or well logging, and the use of laboratory experiments limits the possibility of obtaining a continuous profile for the E_{dyn} along the whole wellbore. On the other hand, the vertical resolution of the logging tool and the interference between the different formations significantly influence the accuracy of the well logging data.

$$E_{dyn} = \frac{\rho V_s^2 \left(3V_P^2 - 4V_s^2\right)}{V_P^2 - V_s^2}, \quad (1)$$

where ρ is the bulk density of the rock (g/cm3), V_S is the shear wave velocity (km/s), and V_P is the compressional wave velocities (km/s).

Machine learning (ML) models were utilized successfully to estimate different parameters and to solve issues related to different aspects of petroleum engineering (Mahmoud et al., 2017; Ahmed et al., 2019; Mahmoud et al., 2020a; Mahmoud et al., 2020b; Al-Abduljabbar et al., 2021; Mahmoud et al., 2021a; Marquez, 2021; Noufal et al., 2021). In this study, the $E_{d\text{-}yn}$ was correlated with the real-time measurable drilling parameters to enable real-time prediction of E_{dyn} using three ML algorithms, namely, random forest (RF), adaptive neuro-fuzzy inference system (ANFIS-SC), and support vector regression (SVR).

2 Methodology

In this study, three ML models, namely, RF, ANFIS-SC, and SVR, were optimized to estimate E_{dyn} from the drilling parameters, i.e., standpipe pressure (SPP), torque, drillpipe rotation speed (DSR), drilling fluid flow rate, weight-on-bit (WOB), and rate of penetration (ROP). Since these drilling parameters are obtained from the surface sensors in real-time during the drilling operation, their use could enable evaluation of the E_{dyn} on a real-time basis.

TABLE 1 Different correlations suggested by previous studies for E_{st} estimation.

Author/s	Empirical correlation	Input	Square correlation of coefficient	No. of data point	Rock type/s
Eissa and Kazi (1988)	$\log(E_{st}) = 0.77 \log(E_{dyn}) + 0.02$	Dynamic and static Young's modulus	0.92	76	NA
Bradford et al. (1998)	$E_{st} = 0.0018\, E_{dyn}^{2.7}$	Dynamic Young's modulus	NA	10	Sandstones and shales
Horsrud, (2001)	$E_{st} = 0.076\, V_P^{3.23}$	Acoustic P-wave velocity	0.99	14	Shale
Lashkaripour, (2002)	$E_{st} = 0.103^{*}\sigma_c^{1.086}$	UCS	0.807	NA	Mudstone
Ameen et al. (2009)	$E_{st} = 0.541\, E_{dyn} + 12.852$	Dynamic Young's modulus	0.6	400	Carbonate
Martínez-Martínez et al. (2012)	$E_{st} = \frac{1.263\, E_{dyn}}{3.8\alpha_s^{-0.68}}$	Dynamic and static Young's modulus	NA	60	Carbonate rocks
	α_s ultrasonic spatial attenuation				
Brotons et al. (2014)	$E_{st} = 0.867\, E_{dyn} - 2.085$	Dynamic Young's modulus	0.96	24	Calcarenite stone
Najibi et al. (2015)	$E_{st} = 0.014\, E_{dyn}^{1.96}$	Dynamic Young's modulus and V_P	0.87–0.9	45	Limestone
	$E_{st} = 0.169\, V_P^{3.324}$				
Ghafoori et al. (2018)	$E_{st} = 0.022\, E_{dyn}^{1.774}$	Dynamic Young's modulus	0.912	60	Limestone rocks
Feng et al. (2019)	$E_{st} = 0.81\, E_{dyn} - 13.88$	Dynamic Young's modulus	0.70–0.92	18	Tight sandstone and siltstone

TABLE 2 Statistical parameters for the training data.

Statistical parameter	WOB, Klb_f	SPP, psi	Torque, $Kft.lb_f$	ROP, ft/hr	DSR, rpm	Flow rate, gpm
Minimum	1.9	2237	4.4	35	92	639
Maximum	24	3,008	11	108	160	853
Median	11	2616	7.1	70	134	700
Standard deviation	7.0	191	1.7	17	15	74

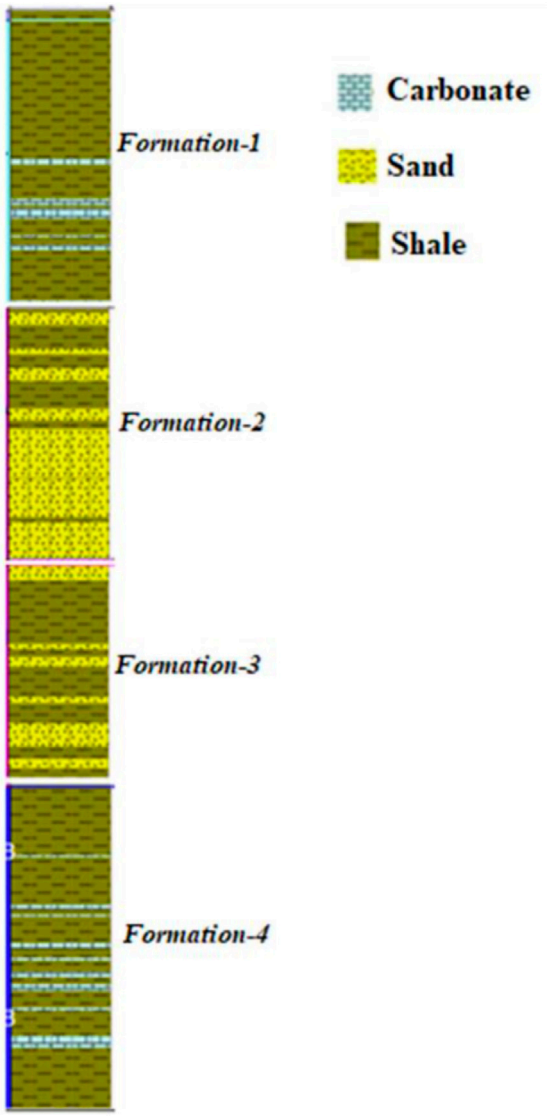

FIGURE 1
Lithology column for Well-A.

TABLE 3 Optimum ML algorithms design parameters for TOC estimation.

RF	
Number of decision trees	100
Maximum depth of the trees	11
Minimum number of the observations	2
Maximum number of inputs	Log2
ANFIS-SC	
Cluster radius	0.3
Number of iterations	300
SVR	
Verbose	1.0
Regression factor	102
Epsilon	10–5
Lambda	10–5
Kernel	Gaussian low
Kernel option	5

2.1 Date description

The drilling parameters and their corresponding E_{dyn} values considered in this work were collected from three different wells; all wells are located in the same oil field from the Middle East. A total of 2054, 871, and 2912 datasets from Well-A, Well-B, and Well-C, respectively, were used to train the ML models on estimating E_{dyn}. Well-A's data were used to learn the ML models, as indicated in Figure 1, Well-A has complex lithology which consists of four formations of sand, shale, and carbonate.

Table 2 lists the statistical features of the training data, which shows the applicable range of the optimized ML models. To

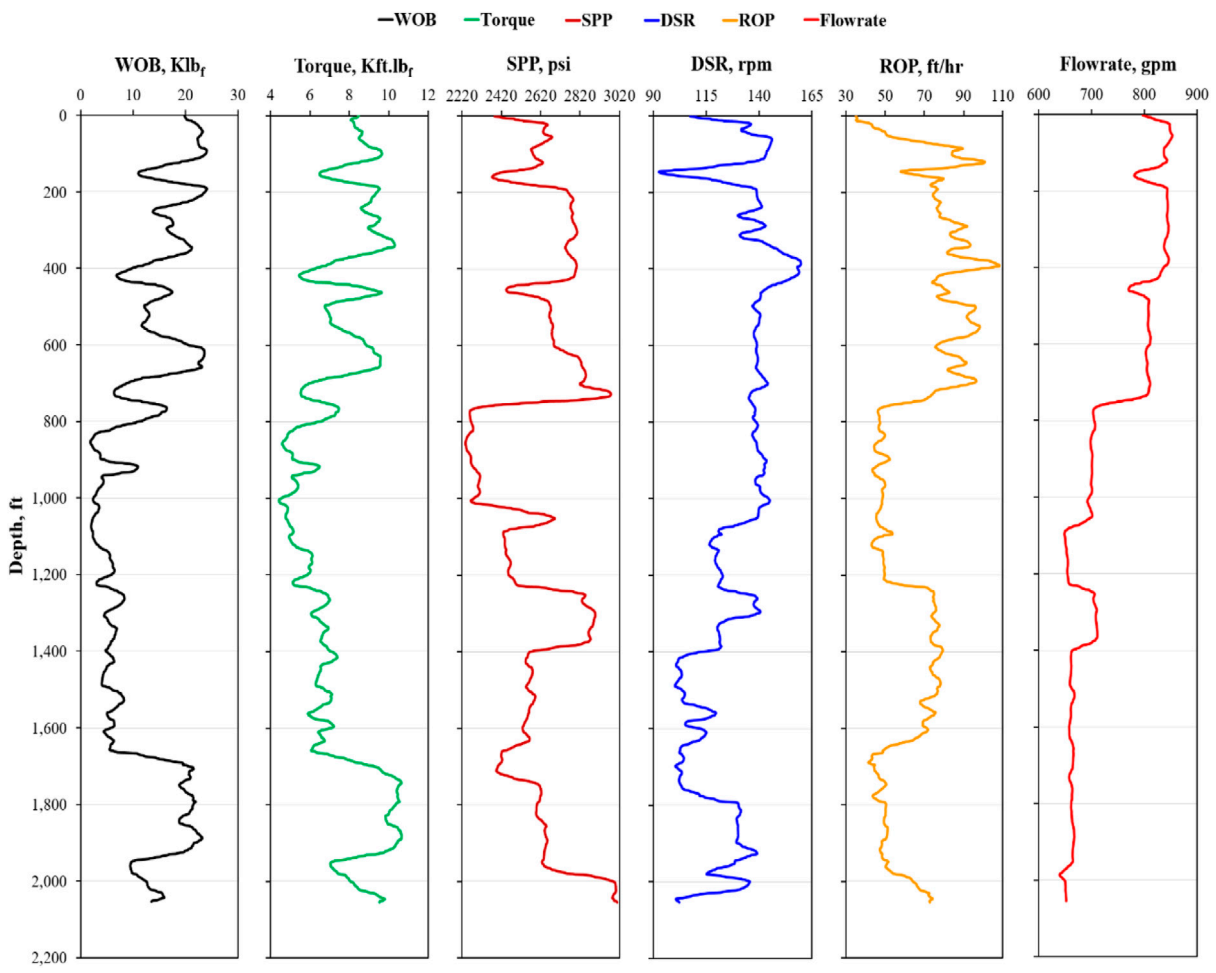

FIGURE 2
Input data used to learn the ML models were collected from Well-A.

ensure the high accuracy of the E_{dyn} with the optimized ML models, the drilling data used to predict the E_{dyn} must be within the range shown in Table 2.

2.1 Concepts of machine learning models

In total, three machine learning models were used in this work. The first model is the random forest (RF) which is a kind of ensemble model applicable to solve both regression and classification problems. In this model, hundreds or thousands decision trees are combined and trained on a slightly different set of observations. Then, in a process called bootstrapping, the splitting nodes of each tree considered only a limited number of input variables to decrease the variance and enhance the predictability of the algorithm (Efron, 1982). Finally, prediction through RF is achieved by averaging the predictions of all trees. RF was successfully applied to solve problems in petroleum engineering (Alsaihati et al., 2021; Osman et al., 2021).

The second model is the adaptive neuro-fuzzy inference system with subtractive clustering (ANFIS-SC). The adaptive neuro-fuzzy inference system (ANFIS) was developed in the early 1990s as a combination of artificial neural networks and fuzzy interference systems (Jang, 1991; Jang, 1993). This way, the ANFIS system could combine the advantages of both neural networks and fuzzy logic in a single model, and it is used mainly for classification purposes, as well as for regression problem. The subtractive clustering is used to group the data based on its potential density to identify the cluster center compared to the surrounding data points. Recently, ANFIS-SC showed high accuracy in solving petroleum

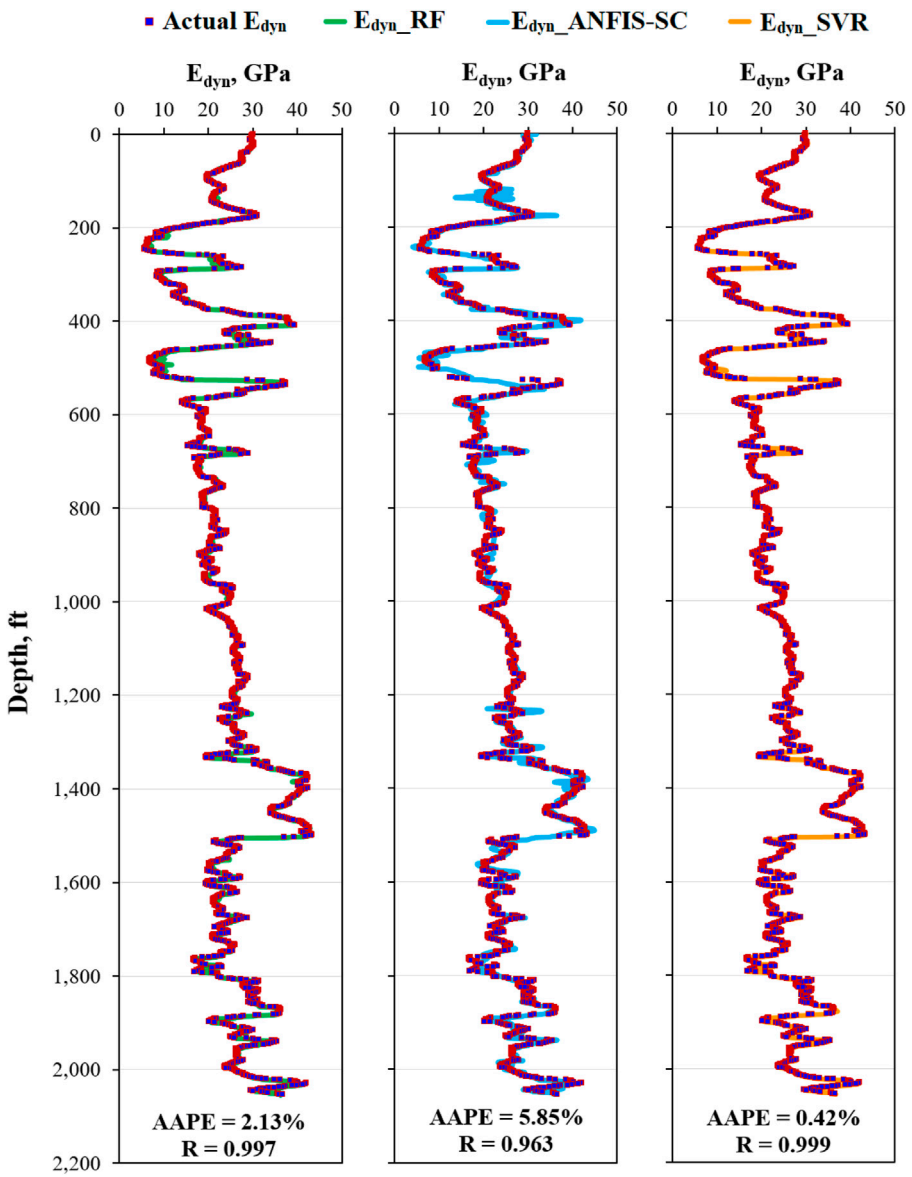

FIGURE 3
Actual and assessed E_{dyn} by the RF, ANFIS-SC, and SVR models for the 2054 training data points of Well-A.

engineering-related problems (Mahmoud et al., 2021b; Gamal et al., 2021).

The third model is support vector regression (SVR) which works based on the principles of the support vector machine (SVM) developed by Vapnik, 1998. The SVM was developed as a classification model, while SVR could be used to solve regression problems. Several previous studies showed the high accuracy of the SVR to identify different parameters related to the petroleum industry (Mahmoud et al., 2020c; Mahmoud et al., 2022).

2.3 Learning the machine learning models

The ML models were trained and optimized in this work using the 2057 datasets of different input parameters collected from Well-A. These inputs are plotted in Figure 2 with the change of depth. To investigate the performance of the different design parameters of the RF, ANFIS-SC, and SVR algorithms in predicting E_{dyn}, sensitivity analysis was performed on different combinations of these design parameters.

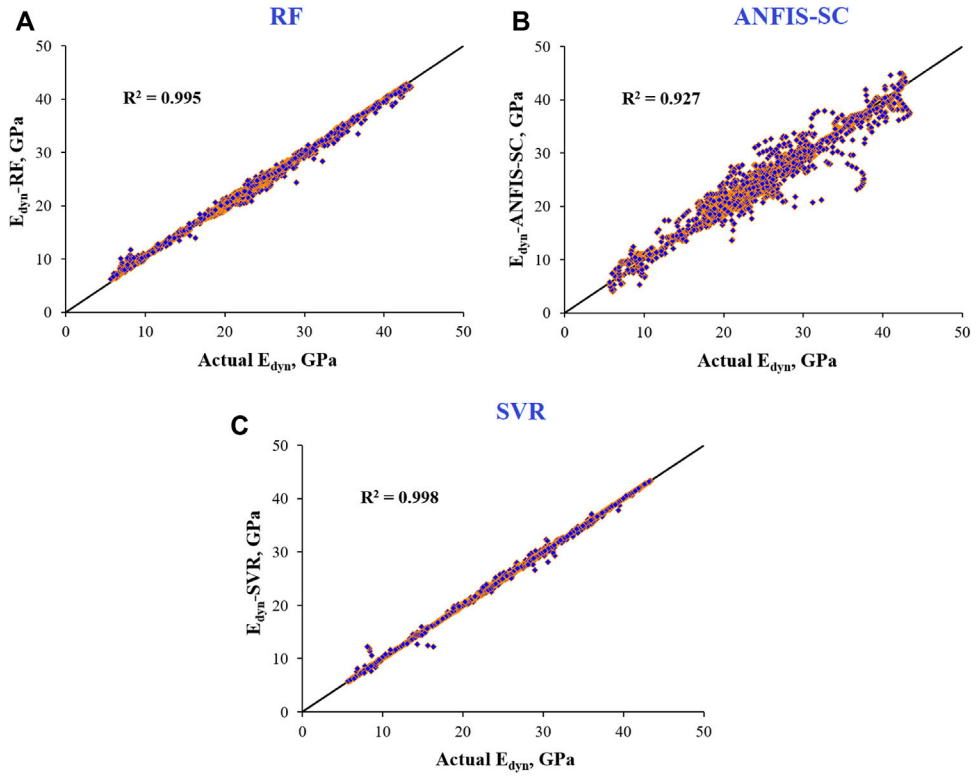

FIGURE 4
Actual and assessed E_{dyn} by the **(A)** RF, **(B)** ANFIS-SC, and **(C)** SVR models for the 2054 training data points of Well-A.

The RF model was optimized on its design parameters of the optimum number of decision trees, the maximum depth of the trees, the minimum number of observations, and the maximum number of inputs. The results showed that the RF model built with 100 decision trees, with a maximum depth of trees of 11, minimum number of observations of 2, and maximum number of inputs of log2, was the best in estimating the E_{dyn} from the surface measurable drilling parameters.

Two design parameters of ANFIS-SC were optimized, namely, cluster radius and number of iterations. The use of cluster radius from 0.2 to 0.7 was evaluated with an increment of 0.05, while the use of iterations from 100 to 1,000 iterations was investigated. The results indicated that the optimum cluster radius was 0.3 when 300 iterations were considered to accurately predict the E_{dyn}.

The SVR model was optimized for its design parameters of the kernel, kernel option, lambda, verbose, regression factor, and epsilon. The optimized SVR model was constructed with the "Gaussian low" kernel, kernel option of 5.0, lambda of 10^{-5}, verbose of 1.0, regression factor of 10^{2}, and epsilon of 10^{-5}.

To ensure evaluation of the performance of all design parameter combinations for the different ML models considered in this study, inserted *for* loops built in MATLAB software were used to optimize these parameters. Then, the optimum parameter combination was considered the one that predicted the E_{dyn} with the lowest average absolute percentage error (AAPE) and highest correlation coefficient (R). The optimum parameters for all optimized models are listed in Table 3.

To avoid the model's overfitting while training, the training data were subdivided into two subgroups, one considered for training (85% of the data) and the other group (15% of the data) was used for validation. The mean square errors for the training and validation data were observed during model training and as a function of the number of trials. These errors were decreasing with the number of trials until the model started memorizing the data because of overfitting, where the error for validation data started increasing with the number of trials, while the error for training data is still decreasing. To avoid overfitting, the optimum number of trials used to train all the ML models was then chosen as that before the validation error started increasing.

2.4 Evaluation of the accuracy of optimized models

After optimizing the ML models, they were tested using 871 data points obtained from the second well (Well-B), and finally, 2912 data points gathered from Well-C were considered for the model's' validation.

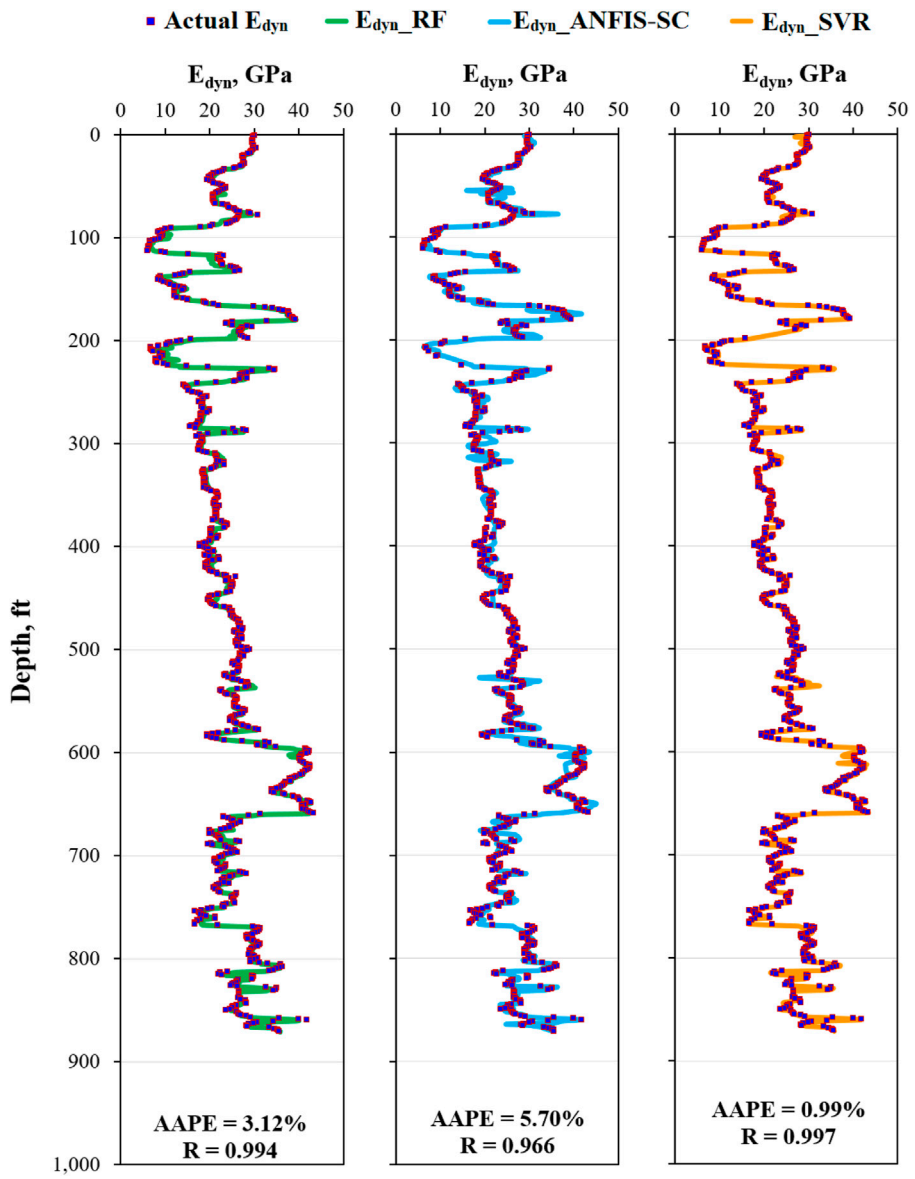

FIGURE 5
Actual and assessed E_{dyn} by the optimized RF, ANFIS-SC, and SVR models for the 871 testing data points of Well-B.

3 Results

3.1 Optimizing the RF, ANFIS-SC, and SVR models

The RF, ANFIS-SC, and SVR models were learned to assess E_{dyn} from the drilling data. The models were learned on the 2054 datasets of Well-A. Figure 3 and Figure 4 compare the actual and assessed E_{dyn} in Well-A, respectively. The ideal matching of the actual E_{dyn} with these predicted with the RF, ANFIS-SC, and SVR models as indicated in Figure 3 emphasizes the high precision of the optimized RF, ANFIS-SC, and SVR models, which predicted the E_{dyn} with AAPEs of 2.13%, 5.85%, and 0.42%, and Rs of 0.997, 0.963, and 0.999, respectively.

The cross-plots of Figure 4 also show that all the points fall in the vicinity of the 45° line, which also assures the high prediction reliability of the optimized RF, ANFIS-SC, and SVR models. As shown in Figure 4B, the coefficient of determination (R^2) between the actual and estimated E_{dyn} is 0.986. Previous results indicated that in terms of accuracy, the model could be arranged as SVR, RF, and ANFIS-SC.

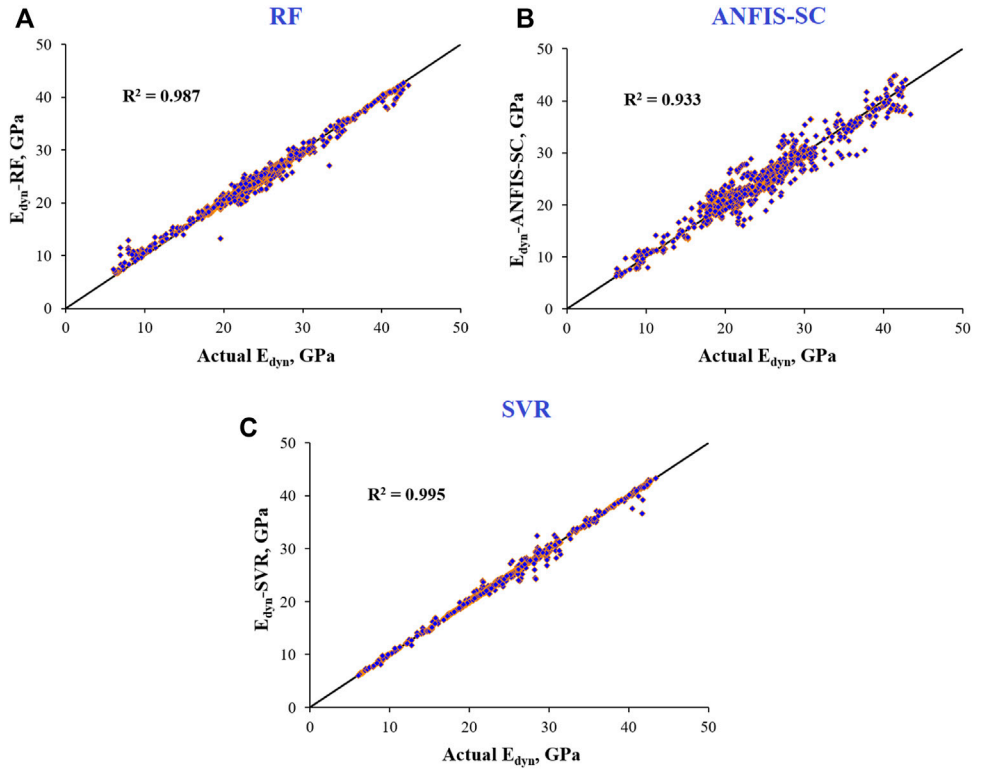

FIGURE 6
Cross-plots of the actual and assessed E_{dyn} by the optimized **(A)** RF, **(B)** ANFIS-SC, and **(C)** SVR models for the 871 testing data points of Well-B.

3.2 Training the machine learning models

The RF, ANFIS-SC, and SVR models optimized in this study were then tested for E_{dyn} assessment using Well-B data. Figure 5 and Figure 6 compare the actual and estimated E_{dyn} in Well-B, respectively. Figure 5 shows that there is a perfect matching of the actual and evaluated E_{dyn}, where the E_{dyn} was predicted with AAPEs of 3.12%, 5.70%, and 0.99%, and Rs of 0.994, 0.966, and 0.997, using the learned RF, ANFIS-SC, and SVR models, respectively.

As indicated in the cross-plots of Figure 6, all the points fall in the vicinity of the 45° line, which assures the high precision of the optimized RF, ANFIS-SC, and SVR models. The E_{dyn} in the testing well was assessed with R^2 of 0.987 using the RF model, 0.933 using the ANFIS-SC model, and 0.995 using the SVR model. Again, for the testing data, the optimized SVR model outperformed the other models in assessing the E_{dyn}, followed by the RF model and then the ANFIS-SC model.

3.3 Validating the optimized random forest, ANFIS-SC, and support vector regression models

The optimized ML models were validated on the 2912 datasets of Well-C. Figure 7 and Figure 8 show the prediction accuracy of these models on evaluating E_{dyn} for Well-C's data. Figure 7 shows that the optimized SVR model was the most accurate among all models optimized in this work, and it assessed the E_{dyn} accurately with a small AAPE of only 1.03% and an R of 0.998. The optimized RF model was the second most accurate, and it determined the E_{dyn} with an AAPE and R of 3.64% and 0.990, respectively. The least precise model was the ANFIS-SC which assessed the E_{dyn} with an AAPE of 6.74% and R of 0.963.

Visual comparison of Figure 8 also confirmed the optimized RF, ANFIS-SC, and SVR models evaluated the E_{dyn} for the data of Well-C with R^2s of 0.980, 0.928, and 0.996, respectively. This result also indicates the high

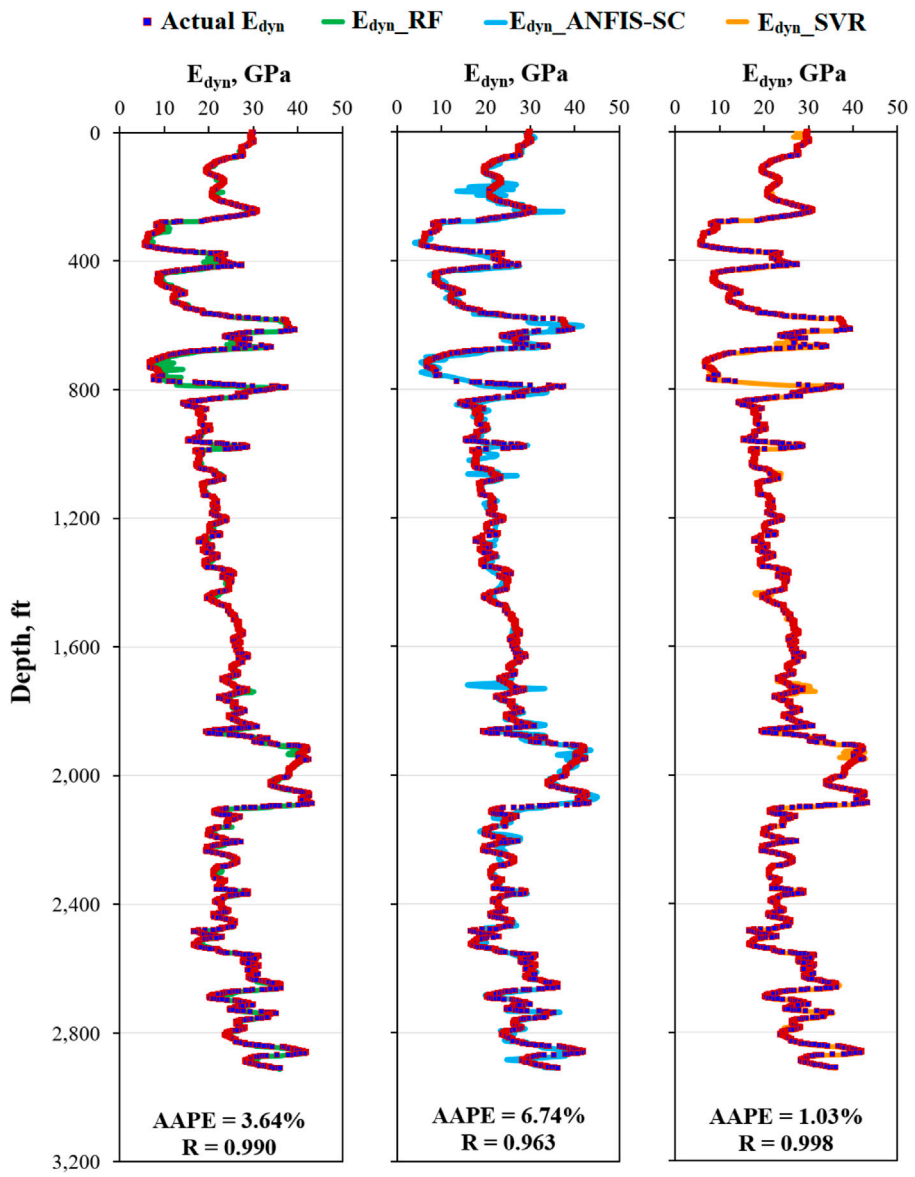

FIGURE 7
Actual and assessed E_{dyn} by the optimized RF, ANFIS-SC, and SVR models, for the 2912 validation data points of Well-C.

reliability of the optimized models in evaluating the E_{dyn} from the surface measurable drilling parameters only.

3.4 Comparing the precision of the random forest, ANFIS-SC, and support vector regression models

Figure 9 compares the accuracy power of the optimized models of RF, ANFIS-SC, and SVR on assessing the E_{dyn} for training, testing, and validation data through evaluation of the accuracy measures of the AAPE, R, and R^2. As indicated in Figure 9A, the SVR model estimated the E_{dyn} with the lowest AAPE for training, testing, and validation data, followed by the RF model, and then the least accurate model was ANFIS-SC.

Now, considering only the validation data of Well-C and the three measures of accuracy (Figure 9B), they also confirmed the high prediction power of the optimized SVR, which estimated the E_{dyn} with the lowest AAPE of 1.03% and the highest R and R^2 of 0.988 and 0.996, respectively.

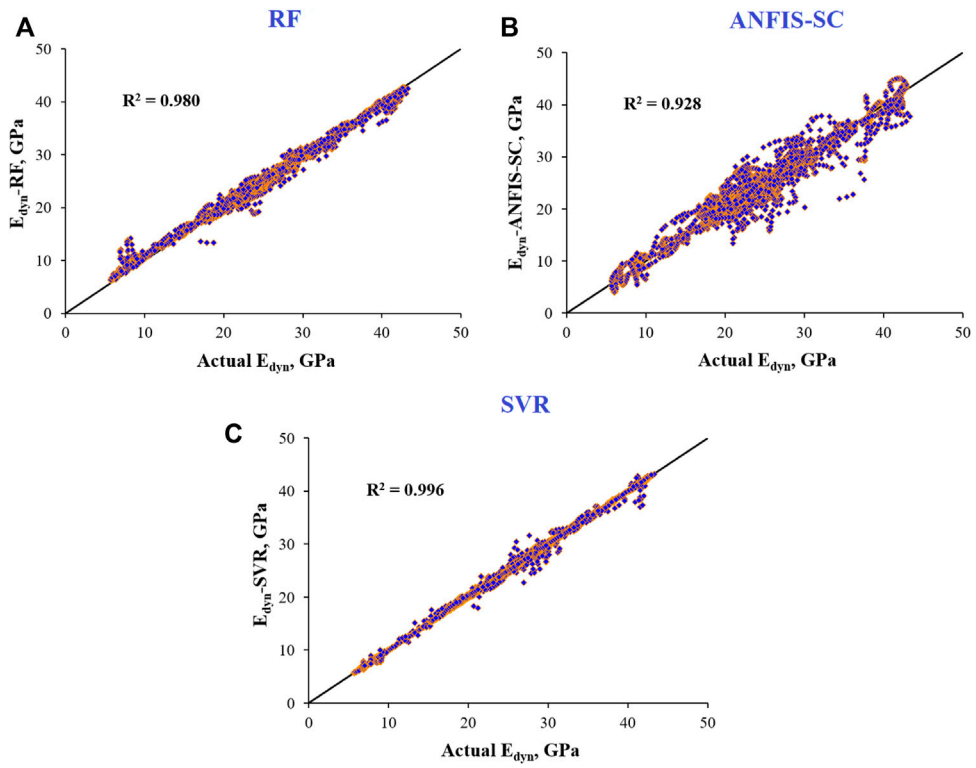

FIGURE 8
Cross-plots of the actual and assessed E_{dyn} by the optimized **(A)** RF, **(B)** ANFIS-SC, and **(C)** SVR models for the 2912 validation data points of Well-C.

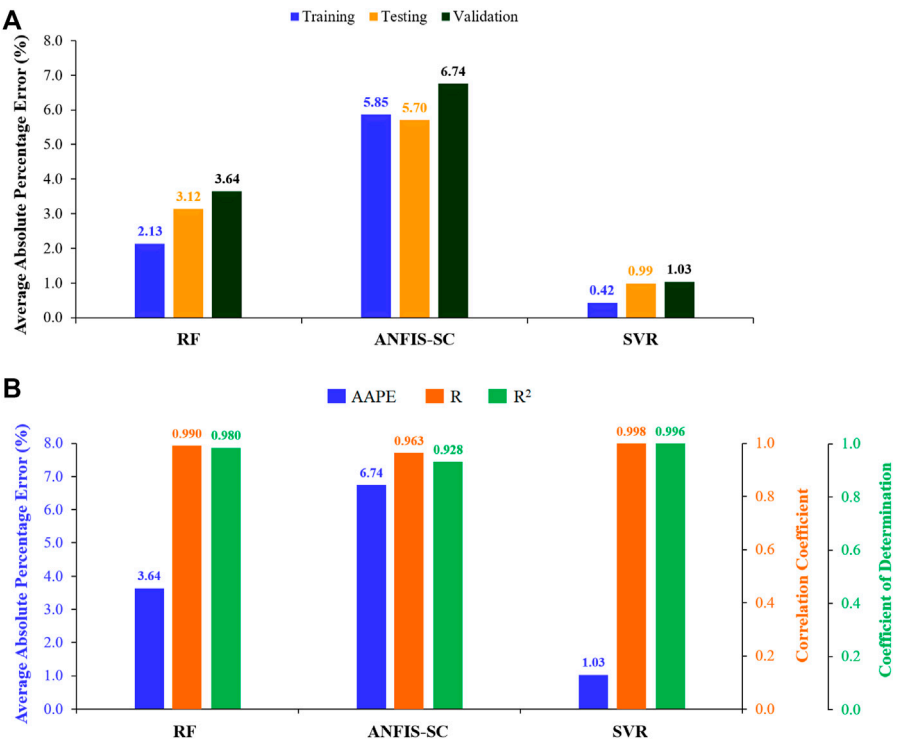

FIGURE 9
Comparison of the prediction accuracy of the optimized RF, ANFIS-SC, and SVR models; **(A)** AAPE for the training, testing, and validation data; and **(B)** the AAPE, R, and R^2 for the validation data of Well-C.

The results showed the high precision of the optimized ML models in estimating the E_{dyn} from the surface measurable drilling parameters; the use of these parameters enabled the possibility of real-time prediction of the E_{dyn}.

4 Conclusion

Three ML models, namely, RF, ANFIS-SC, and SVR, were optimized for real-time assessment of the E_{dyn} from the real-time available drilling parameters only. The ML models were optimized on 2054 datasets of the different input parameters and their corresponding E_{dyn} and then tested and validated on 871 and 2912 datasets from another two wells. The following conclusion can be drawn based on this study:

- The three ML models accurately predicted the E_{dyn} in the three oil wells considered in this study.
- The optimized SVR model was more accurate than the RF and ANFIS-SC models in evaluating the E_{dyn} in all three wells.
- For the validation data, E_{dyn} was assessed accurately with low AAPEs of 3.64%, 6.74%, and 1.03% using RF, ANFIS-SC, and SVR models, respectively.
- The use of the surface measurable drilling parameters enabled real-time assessment of the E_{dyn}.

Data availability statement

The original contributions presented in the study are included in the article; further inquiries can be directed to the corresponding author.

Author contributions

Conceptualization, SE; methodology, AM and HG; validation, AM, HG, and WC; formal analysis, AM and WC; writing—original draft preparation, AM; writing—review and editing, AM, SE, and WC; and supervision, SE.

Acknowledgments

The authors wish to acknowledge King Fahd University of Petroleum and Minerals for providing research facilities and permitting the publication of this work.

Conflict of interest

The authors declare that the research was conducted in the absence of any commercial or financial relationships that could be construed as a potential conflict of interest.

Publisher's note

All claims expressed in this article are solely those of the authors and do not necessarily represent those of their affiliated organizations, or those of the publisher, the editors, and the reviewers. Any product that may be evaluated in this article, or claim that may be made by its manufacturer, is not guaranteed or endorsed by the publisher.

References

Ahmed, S. A., Mahmoud, A. A., Elkatatny, S., Mahmoud, M., and Abdulraheem, A. (2019). "Prediction of pore and fracture pressures using support vector MachineMarch," in Proceeding of the Paper IPTC-19523-MS Presented at the 2019 International Petroleum Technology Conference, Beijing, China, 26–28. doi:10.2523/IPTC-19523-MS

Al-Abduljabbar, A., Mahmoud, A. A., and Elkatatny, S. (2021). Artificial neural network model for real-time prediction of the rate of penetration while horizontally drilling natural gas-bearing sandstone formations. *Arab. J. Geosci.* 14, 117. doi:10.1007/s12517-021-06457-0

Alsaihati, A., Elkatatny, S., Mahmoud, A. A., and Abdulraheem, A. (2021). Use of machine learning and data analytics to detect downhole abnormalities while drilling horizontal wells, with real case study. *J. Energy Resour. Technol.* 143. doi:10.1115/1.4048070

Ameen, M. S., Smart, B. G. D., Somerville, J. M., Hammilton, S., and Naji, N. A., 2009. Predicting rock mechanical properties of carbonates from wireline logs (A case study: Arab-D reservoir, Ghawar field, Saudi Arabia). *Mar. Pet. Geol.* 26, 430–444. doi:10.1016/j.marpetgeo.2009.01.017

Asef, M. R., and Farrokhrouz, M. (2017). A semi-empirical relation between static and dynamic elastic modulus. *J. Pet. Sci. Eng.* 157, 359–363. doi:10.1016/j.petrol.2017.06.055

Barree, R. D., Gilbert, J. V., and Conway, M. (2009). "Stress and rock property profiling for unconventional reservoir stimulation," in The SPE Hydraulic Fracturing Technology Conference, The Woodlands, Texas, January 19-21, 2009. doi:10.2118/118703-MS

Bradford, I. D. R., Fuller, J., Thompson, P. J., and Walsgrove, T. R. (1998). "Benefits of assessing the solids production risk in a north sea reservoir using elastoplastic modelling", in The SPE/ISRM Rock Mechanics in Petroleum Engineering, Trondheim, Norway, July 8-10, 1998. doi:10.2118/47360-MS

Brotons, V., Tomás, R., Ivorra, S., Grediaga, A., Martínez-Martínez, J., Benavente, D., et al. (2016). Improved correlation between the static and dynamic elastic modulus of different types of rocks. *Mat. Struct.* 49, 3021–3037. doi:10.1617/s11527-015-0702-7

Brotons, V., Tomás, R., Ivorra, S., and Grediaga, A. (2014). Relationship between static and dynamic elastic modulus of calcarenite heated at different temperatures: The san julián's stone. *Bull. Eng. Geol. Environ.* 73, 791–799. doi:10.1007/s10064-014-0583-y

Efron, B. (1982). *The jackknife, the bootstrap and other resampling plans*. Stanford, CA: SIAM.

Eissa, E. A., and Kazi, A. (1988). Relation between static and dynamic Young's moduli of rocks. *Int. J. Rock Mech. Min. Sci. Geomechanics Abstr.* 25, 479–482. doi:10.1016/0148-9062(88)90987-4

Feng, C., Wang, Z., Deng, X., Fu, J., Shi, Y., Zhang, H., et al. (2019). A new empirical method based on piecewise linear model to predict static Poisson's ratio via well logs. *J. Pet. Sci. Eng.* 175, 1–8. doi:10.1016/j.petrol.2018.11.062

Fjaer, E., Holt, R. M., Raaen, A. M., and Horsrud, P. (2008). *Petroleum related rock mechanics*. Netherlands: Elsevier Science. Volume 53.

Gamal, H., Elkatatny, S., and Mahmoud, A. A. (2021). Machine learning models for generating the drilled porosity log for composite formations. *Arab. J. Geosci.* 14, 2700. doi:10.1007/s12517-021-08807-4

Ghafoori, M., Rastegarnia, A., and Lashkaripour, G. R., (2018). Estimation of static parameters based on dynamical and physical properties in limestone rocks. *J. Afr. Earth Sci.* 137, 22–31. doi:10.1016/j.jafrearsci.2017.09.008

Hammah, R., Curran, J., and Yacoub, T. (2006). *The influence of Young's modulus on stress modelling results*. Golden, Colorado: 41st U.S. Symp. Rock Mech. Golden Rocks 2006.

Horsrud, P. (2001). Estimating mechanical properties of shale from empirical correlations. *SPE Drill. Complet* 16, 68–73. doi:10.2118/56017-PA

Jang, J.-S. R. (1993). Anfis: Adaptive-network-based fuzzy inference system. *IEEE Trans. Syst. Man. Cybern.* 23 (3), 665–685. doi:10.1109/21.256541

Jang, J.-S. R. (1991). "Fuzzy modeling using generalized neural networks and kalman filter algorithm (PDF)," in The Proceedings of the 9th National Conference on Artificial Intelligence, Anaheim, CA, USA, 14–19 July. 2, 762–767.

Karagianni, A., Karoutzos, G., Ktena, S., Vagenas, N., Vlachopoulos, I., Sabatakakis, N., et al. (2017). Elastic properties of rocks. *geosociety.* 43, 1165. doi:10.12681/bgsg.11291

King, M. S., 1983. Static and dynamic elastic properties of rocks from the Canadian shield. *Int. J. Rock Mech. Min. Sci. Geomechanics Abstr.* 20, 237–241. doi:10.1016/0148-9062(83)90004-9

Labudovic, V. (1984). The effect of Poisson's ratio on fracture height. *J. Pet. Technol.* 36, 287–290. doi:10.2118/10307-PA

Lacy, L. L. (1997). "Dynamic rock mechanics testing for optimized fracture designs," in proceeding of the SPE Annu. Tech. Conf. Exhib. doi:10.2118/38716-MS

Lashkaripour, G. R. (2002). Predicting mechanical properties of mudrock from index parameters. *Bull. Eng. Geol. Environ.* 61, 73–77. doi:10.1007/s100640100116

Mahmoud, A. A., Elkatatny, S., Abduljabbar, A., Moussa, T., Gamal, H., and Al Shehri, D. (2020b). "Artificial neural networks model for prediction of the rate of penetration while horizontally drilling carbonate formations," in Proceedings of the 54th US Rock Mechanics/Geomechanics Symposium, 28 June - 1 July.

Mahmoud, A. A., Elkatatny, S., Abdulraheem, A., Mahmoud, M., Ibrahim, O., and Ali, A. (2017). "New technique to determine the total organic carbon based on well logs using artificial neural network (white box)," in Proceeding of the Paper SPE-188016-MS Presented at the 2017 SPE Kingdom of Saudi Arabia Annual Technical Symposium and Exhibition, Saudi Arabia, April 24–27, 2017 (Dammam), 24–27. doi:10.2118/188016-MS

Mahmoud, A. A., Elkatatny, S., and Al Shehri, D. (2022). "Estimation of the static young's modulus for sandstone reservoirs using support vector regression," in proceeding of the Paper presented at the International Petroleum Technology Conference, Riyadh, Saudi Arabia, 21–23. doi:10.2523/IPTC-22071-MS

Mahmoud, A. A., Elkatatny, S., and Al-Abduljabbar, A. (2021b). Application of machine learning models for real-time prediction of the formation lithology and tops from the drilling parameters. *J. Petroleum Sci. Eng.* 203, 108574. doi:10.1016/j.petrol.2021.108574

Mahmoud, A. A., Elkatatny, S., and Al-Shehri, D. (2020c). Application of machine learning in evaluation of the static Young's modulus for sandstone formations. *Sustainability* 12 (5), 1880. doi:10.3390/su12051880

Mahmoud, A. A., Elkatatny, S., Alsabaa, A., and Al Shehri, D. (2020a). "Functional neural networks-based model for prediction of the static young's modulus for sandstone formations," in Proceedings of the 54th US Rock Mechanics/Geomechanics Symposium, 28 June - 1 July.

Mahmoud, A. A., Gamal, H., Mutrif, O., and Elkatatny, S. (2021a). "Artificial neural networks-based equation for real-time estimation of the dynamic young's modulus," in Proceeding of the Paper presented at the 55th U.S. Rock Mechanics/Geomechanics Symposium, Virtual.

Marquez, F. J. (2021). "Drilling optimization applying machine learning regression algorithms," in Proceeding of the Paper presented at the Offshore Technology Conference, Virtual and Houston, Texas, 16–19. doi:10.4043/30934-MS

Martínez-Martínez, J., Benavente, D., and García-del-Cura, M. A. (2012). Comparison of the static and dynamic elastic modulus in carbonate rocks. *Bull. Eng. Geol. Environ.* 71, 263–268. doi:10.1007/s10064-011-0399-y

Najibi, A. R., Ghafoori, M., Lashkaripour, G. R., and Asef, M. R. (2015). Empirical relations between strength and static and dynamic elastic properties of Asmari and Sarvak limestones, two main oil reservoirs in Iran. *J. Pet. Sci. Eng.* 126, 78–82. doi:10.1016/j.petrol.2014.12.010

Nes, O.-M., Fjær, E., Tronvoll, J., Kristiansen, T. G., and Horsrud, P. (2005). "Drilling time reduction through an integrated rock mechanics analysis," in Proceeding of the SPE/IADC Drill. Conf, Amsterdam, Netherlands, February 23–25, 2009. doi:10.2118/92531-MS

Noufal, A., Sreekantan, J., Belmeskine, R., Amri, M., and Benaichouche, A. (2021). "Machine learning in computer vision software for geomechanics modeling," in proceeding of the Paper presented at the Abu Dhabi International Petroleum Exhibition & Conference, Abu Dhabi, UAE, 15 – 18 November. doi:10.2118/208049-MS

Osman, H., Ali, A., Mahmoud, A. A., and Elkatatny, S. (2021). Estimation of the rate of penetration while horizontally drilling carbonate formation using random forest. *J. Energy Resour. Technol.* 143. doi:10.1115/1.4050778

Vapnik, V. (1998). *Statistical learning theory*. New York, NY, USA: Wiley. 978-0471030034.